NATIONAL ADVISORY COMMITTEE FOR AERONAUTICS

TECHNICAL NOTE 2041

AN EXPERIMENTAL INVESTIGATION OF THE NACA 63_1-012 AIRFOIL SECTION WITH LEADING-EDGE AND MIDCHORD SUCTION SLOTS

By George B. McCullough and Donald E. Gault

Ames Aeronautical Laboratory
Moffett Field, Calif.

Washington
February 1950

NATIONAL ADVISORY COMMITTEE FOR AERONAUTICS

TECHNICAL NOTE 2041

AN EXPERIMENTAL INVESTIGATION OF THE NACA 63_1-012 AIRFOIL SECTION WITH LEADING-EDGE AND MIDCHORD SUCTION SLOTS

By George B. McCullough and Donald E. Gault

SUMMARY

A previous investigation of boundary-layer control employing a two-dimensional model of the NACA 63_1-012 airfoil section demonstrated the ability of a single suction slot near the leading edge to increase maximum lift. It was believed possible, however, that the complete stall may have resulted from leading-edge separation because of the inability of the nose suction to hold the flow on the surface. To investigate the effectiveness of the nose slot at higher values of lift, a second suction slot was added near the midchord station of the model. This report is concerned with the results obtained with the two slots operating simultaneously.

It was found that suction through the midchord slot in conjunction with the nose slot resulted in substantial gains in the maximum lift over that obtainable with nose suction alone. The effectiveness of the boundary-layer control increased with increased flow through the nose and midchord slots. The exact nature of the section stalling characteristics could not be determined because of a breakdown of the flow over the model near maximum lift, which was thought to be caused by inflow from the wind-tunnel-wall boundary layer.

The data presented include force and moment measurements, pressure distributions, and boundary-layer-velocity profiles obtained at Reynolds numbers of 4.1 and 5.8 million.

INTRODUCTION

Wing sections suitable for high-speed application usually stall at relatively low values of maximum lift coefficient because of separation of the flow near the leading edge. The occurrence of this type of stall may introduce serious difficulties to the low-speed operation of airplanes. It has been demonstrated that the undesirable effects of leading-edge separation may be overcome, in part at least, by suitable flaps at the leading edge of the wing. Another solution which has been suggested is the application of boundary-layer control near the leading edge.

An investigation of the latter method has been completed and is reported in reference 1. The airfoil section employed was the NACA 63_1-012. This section was chosen because a preliminary investigation of its boundary-layer characteristics showed that the flow separated from the leading edge completely and abruptly before the onset of turbulent separation at the trailing edge. Boundary-layer suction through a single slot in the upper surface near the leading edge proved to be effective in delaying separation of flow from the leading edge, at least until after the establishment of turbulent separation at the trailing edge. The maximum lift was increased about one-third above that of the basic airfoil section. It could not be demonstrated, however, that the stall was entirely the result of turbulent separation. It was believed possible that the nose suction slot may have been incapable of holding the flow on the surface at larger values of lift, and that the complete stall may have resulted from a combination of laminar and turbulent separation.

In order to test the capability of the nose slot at larger values of lift, a second investigation – the subject of this report – was made. The original suction airfoil model was revised by the addition of a suction slot near midchord. It was expected that the midchord slot, by delaying separation of the turbulent boundary layer, would permit the attainment of larger values of maximum lift. The associated pressure minimums and pressure gradients in the vicinity of the nose slot would be more severe than those of the original investigation, and would test the ability of the nose slot to hold the flow on the surface.

No attempt was made to determine the optimum midchord slot for controlling the turbulent boundary layer. (Considerable data on suction slots for controlling turbulent separation already exist.) Instead, the midchord slot was considered simply as a device for imposing more severe conditions on the nose slot.

In order to make the present investigation continuous with that of reference 1, the first nose slot tested was identical with the best slot found in the original investigation. Other nose slots were also tried. The data presented include measurements of lift, drag, pitching moment, and chordwise pressure distribution as well as boundary-layer surveys. The investigation was conducted in the Ames 7- by 10-foot wind tunnel No. 1.

SYMBOLS

The symbols used in this report are defined as follows:

c wing chord, 5 feet

c_{d_o}' section drag coefficient as measured by the wind-tunnel balance system, corrected for jet-boundary effect by the method of reference 2 $\left(\frac{D}{q_o c}\right)$

c_{d_o} section profile drag coefficient as determined from wake surveys, corrected for jet-boundary effect by the method of reference 2 $\left(\frac{D}{q_o c}\right)$

c_l section lift coefficient, corrected for jet-boundary effect by the method of reference 2 $\left(\frac{L}{q_o c}\right)$

c_m section pitching-moment coefficient, corrected for jet-boundary effect by the method of reference 2 $\left(\frac{M}{q_o c}\right)$

c_{q_N} section flow coefficient of nose slot $\left(\frac{Q}{U_o c}\right)$

c_{q_B} section flow coefficient of midchord slot $\left(\frac{Q}{U_o c}\right)$

D drag per unit span, pounds

H boundary-layer-shape parameter $\left(\frac{\delta^*}{\theta}\right)$

L lift per unit span, pounds

M pitching moment per unit span, pound-feet

p_l local static pressure, pounds per square foot

p_o free-stream static pressure, pounds per square foot

P pressure coefficient $\left(\frac{p_l - p_o}{q_o}\right)$

q_o free-stream dynamic pressure $\left(\frac{1}{2}\rho_o U_o^2\right)$, pounds per square foot

Q volume flow through slot, at free-stream density, per unit span, cubic feet per second

R Reynolds number $\left(\frac{U_o c}{\nu}\right)$

u local velocity inside boundary layer, feet per second

U local velocity outside boundary layer, feet per second

U_o free-stream velocity, feet per second

w slot width, feet

x distance from airfoil leading edge measured parallel to chord line, feet

y distance above airfoil measured normal to surface, feet

α_o section angle of attack, corrected for jet-boundary effect by the method of reference 2, degrees

δ total boundary-layer thickness, feet

δ_f flap deflection, degrees

δ^* boundary-layer-displacement thickness, feet $\left[\int_o^\delta \left(1-\frac{u}{U}\right) dy\right]$

θ boundary-layer-momentum thickness, feet $\left[\int_o^\delta \frac{u}{U}\left(1-\frac{u}{U}\right) dy\right]$

ρ_o free-stream mass density, slugs per cubic foot

ν kinematic viscosity, feet squared per second

MODEL AND APPARATUS

Model

A typical section through the model and detailed dimensions of the suction slots are shown in figure 1.

The model was a 5-foot chord, NACA 63_1-012, two-dimensional airfoil equipped with a 27.5-percent-chord plain flap hinged at the chord line. Circular end plates, 6 feet in diameter, attached to the model, formed part of the wind-tunnel floor and ceiling. Two internal plenum chambers provided the ducting for the suction slots. Bench tests of simulated plenum chambers and suction slots indicated that the internal cross-sectional areas were large enough to insure reasonably uniform flow into the slots across the 7-foot span of the model. Flush orifices were provided in the surface of the model for the measurement of pressure distribution.

The nose-slot opening could be closed with a series of narrow, spanwise strips. The strips, shaped to the normal contour of the airfoil section at the outer edges, fitted together snugly so as to prevent leakage between adjoining strips. By removing the strips one at a time, the nose slot could be successively widened without alterations to the model. Slot 1 was 0.48 inch or 0.800-percent chord wide, and was identical with slot 15 described in reference 1. Slot 2 was 0.84 inch or 1.400-percent chord wide, the widest slot investigated.

The center line of the midchord slot was at 51-percent chord. This location was dictated primarily by model construction limitations. A more forward location was impossible due to interference with a hollow steel spar (which also formed part of the rear plenum chamber) in the midsection of the model. It was thought that a more rearward location would have reduced the effectiveness of the slot. The position and width of the midchord slot were not designed to be alterable in the wind tunnel.

Apparatus

The suction required to induce flow into the two slots was provided by two independent centrifugal blowers and ducting systems. Each ducting system was connected to the model through a mercury seal, one above the upper end of the model, and the other below the lower end of the model. This arrangement isolated the model from mechanical forces introduced by the external piping.

The quantity of flow through the slots was calculated from the pressure drop across an orifice meter in each suction line. The air pressure within the two plenum chambers was measured by means of static-pressure tubes in the plenum chambers.

Boundary-layer-velocity profiles were measured by means of small rakes attached to the surface of the model. Each rake consisted of one static-pressure tube and six or more total-pressure tubes. Several sizes of rakes were used, depending on the thickness of the boundary layer. Measurements were made ranging from a few thousandths of an inch to 10 inches above the airfoil surface.

METHOD

The data were obtained while the angle of attack of the model was varied with various constant values of the flow coefficient c_q maintained for each of the two suction slots. Tests were also made with the midchord slot sealed with cellulose tape and suction applied to the nose slot only.

Force measurements were made with the usual wind-tunnel balance system. In addition to the balance-system measurements, the drag was measured by the wake-survey method. Pressure distributions, boundary-layer surveys, and plenum-chamber pressures were recorded photographically from multiple-tube manometers.

Whenever possible, the tests were made with a dynamic pressure of 40 pounds per square foot, which corresponded to a Reynolds number of 5.8 million and a Mach number of 0.167. However, in order to obtain flow coefficients greater than 0.0038 for the nose slot, or 0.0080 for the mid-chord slot, the dynamic pressure was reduced to 20 pounds per square foot, which corresponded to a Reynolds number of 4.1 million and a Mach number of 0.116.

RESULTS AND DISCUSSION

Lift, Drag, and Moment Characteristics

Typical lift, drag, and pitching-moment data for the model with nose slot 2 and the largest suction flow permitted by the apparatus are shown in figure 2. Similar data for the model without suction slots are also shown for comparison. The section drag coefficients c_{d_o}' shown in this figure were computed from readings of the drag balance, and therefore include the tare drag of the circular end plates as well as the sink drag of the boundary-layer flow inducted into the slots (i.e., the component of momentum of the inducted air in the drag direction). The effect of the end plates on the measured values of lift and pitching moment is known to be small.

The external drag coefficient c_{d_o} of the model as evaluated by the wake-survey method is shown in figure 3.

Summary plots showing the variation of maximum section lift coefficient with flow coefficient are presented in figures 4 and 5 for the model with the flap undeflected and deflected 40°, respectively. Data are given for nose slots 1 and 2. Slots of intermediate width, produced by successively removing the strips on the downstream edge of slot 1, were investigated briefly and proved to be inferior to slot 2. Since it was not the purpose of the present investigation to ascertain the optimum leading-edge slot, no data are presented for slots of intermediate width. Slots wider than nose slot 2 were not investigated because of model construction limitations.

The manner of fairing the data in figures 4 and 5, that is, the use of a single curve to join test points obtained for one value of Reynolds number with those obtained for a different value, is open to criticism. A few test points corresponding to intermediate flow coefficients were obtained for both values of Reynolds number. In some cases the agreement was good; in the other cases, larger maximum lift coefficients were obtained for the smaller value of Reynolds number. The scatter was not much greater than that caused by the unsteady flow conditions which existed at maximum lift.

Lift with nose slot only.– The maximum section lift coefficient of the basic airfoil section, as reported in reference 1, was 1.38 with the flap undeflected and 2.03 with the flap deflected 40°. With suction applied to nose slot 1 ($c_{q_N} = 0.0065$), these values were increased to 1.84 and 2.54. As previously mentioned, the nose slot was successively widened during the course of the present investigation. The maximum section lift coefficient increased with increased slot width. The effectiveness of nose slot 2 can be seen in figures 4 and 5. The maximum section lift coefficient ($c_{q_N} = 0.0065$) was 2.00 with the flap undeflected and 2.57 with the flap deflected 40°. It is to be noted, however, that the greater effectiveness of nose slot 2, as compared to nose slot 1, occurred only for the higher values of flow coefficient. Whereas the maximum section lift coefficient of the model with nose slot 1 (and with the narrower slots described in reference 1) appeared to be approaching an ultimate value asymptotically with increasing flow coefficient, the data for nose slot 2 showed a continuous increase of $c_{l_{max}}$ at least up to the largest value of flow coefficient employed in the investigation ($c_{q_N} = 0.0065$). It seems probable, therefore, that greater values of lift coefficient could be attained by further increasing the suction flow into nose slot 2.

It should be mentioned that the increment of lift produced by the suction slot was not solely attributable to the direct effects of boundary-layer control, but was due in part to the pressure difference which existed across the face of the slot. Since, for a given angle of attack, the internal plenum-chamber pressure was less than the external pressure over the portion of the basic airfoil corresponding to the slot opening, an increment of lift resulted which was entirely due to suction. For the angle of attack corresponding to maximum lift of the basic airfoil section with the flap undeflected, it is estimated that the suction pressure necessary to produce a flow coefficient of 0.0065 with nose slot 2 would produce an increment of lift coefficient of the order of 0.05. For narrower nose slots, of course, the increment would be smaller. For the midchord slot, because of smaller pressure differentials, the lift increment is negligible. It is obvious, therefore, that the increments of maximum lift obtained in the present investigation are predominately the result of delaying the flow separation which caused the stall of the basic airfoil section.

Lift with nose slot and midchord slot.– The effectiveness of the midchord slot in conjunction with either nose slot 1 or 2 can also be seen in figures 4 and 5. For all conditions investigated, operation of the midchord slot produced substantial gains in the maximum section lift coefficient. The largest gains were obtained with nose slot 2. With maximum flow into both slots $c_{q_N} = 0.0065$, $c_{q_B} = 0.0115$, values of $c_{l_{max}}$ of 2.39 and 2.87 were obtained with the flap undeflected and deflected 40°. As compared to the basic airfoil, these values represent increments of the maximum section lift coefficient of 1.01 for the model with flap undeflected, and 0.84 with the flap deflected 40°. The corresponding increments with nose slot 1 (reference 1) were 0.46 and 0.51.

The effect of the midchord slot on the variation of lift with angle of attack was substantially the same as that of the nose slot. The linear portion of the lift curve was extended to higher angles of attack, and, consequently, to higher values of the lift coefficient. Although flow into the nose slot caused no change in the angle of attack for zero lift (reference 1), the action of the midchord slot was to reduce the angle of attack for zero lift (fig. 2). This effect, however, was small, amounting to only about 0.5° for the maximum suction flow investigated. For the model with the flap undeflected and with both slots operative, the entire lift curve was displaced, but, with the flap deflected 40°, the lift curve was displaced only near zero lift, and the lift curves with and without suction coincided throughout most of the lift range.

The stall of the model with combined nose and midchord suction was accompanied by irregular flow in the wind tunnel. Visual observation of the action of short tufts of thread glued to the surface showed that separation began at the outer ends of the model near the trailing edge, spreading forward and inward with increasing angle of attack. At the angle of attack for maximum lift, wedge-shaped areas of intermittently separated flow were formed at either end of the model although the flow at the midspan section was relatively steady.

It is believed that this flow condition was caused by the boundary layer of the tunnel floor and ceiling bleeding into the boundary layer of the wing, thereby causing premature turbulent separation of flow from the outer sections of the model and an effective loss of lifting area. If the bleeding action could have been prevented, it is probable that greater values of lift would have been attained before the model stalled completely. For this reason, the values of the maximum lift coefficient given herein are believed to be lower than the true section values.

Drag.- The drag measured by the wind-tunnel balance system, as previously mentioned, included the tare drag of the circular end plates and the sink drag of the flow induced into the suction slots. The sink drag accounted for the greater drag of the suction model shown in figure 2. A second effect of boundary-layer suction, shown by the wake-survey measurements of figure 3, was to reduce the external profile drag of the suction model below that of the basic model. Just the opposite occurred for the model without the midchord slot. It is shown in reference 1 that the external drag of the model with nose slot 1 was, in general, equal to or greater than the profile drag of the basic section. It is evident that the reduction of drag experienced by the model with the midchord suction slot resulted from a thinning of the turbulent boundary layer over the portion of the model downstream of the midchord slot. The net effect, then, of the boundary-layer suction was to increase the total drag because the sink drag was greater than the reduction of profile drag produced by boundary-layer control. (In an idealized system, of course, the sink drag could be exactly offset by preserving the momentum of the inducted air and discharging it in the rearward direction.)

Pitching moment.— The effect of the midchord slot on the pitching moments was small. Since the nose slot alone produced no appreciable effect (reference 1), the slight positive shift of the pitching-moment curve with both slots operating, shown in figure 2, may be attributed to the sink effect of the midchord slot on the chordwise loading. The effect of the reduced thickness of the turbulent boundary layer downstream of the slot would be to produce more negative pitching moments, the opposite effect from that observed.

Pressure Distribution

Some typical pressure distributions are shown in figures 6 and 7 for the model with the flap undeflected and with it deflected 40°. Pressure distributions for the model without suction slots near maximum lift are also shown on these plots. The values of the pressure coefficient P are observed values and have not been corrected to zero Mach number. The negative pressure-coefficient peaks near the nose of the suction model were so great as to extend beyond the range of the ordinate scale. The observed values in this region are tabulated in the plots. The fairing of the pressure coefficients in the vicinity of the midchord slot is more or less arbitrary because of the lack of sufficient pressure orifices to define accurately the location of the stagnation point on the downstream edge of the slot.

It is apparent that the increased lift of the model with combined nose and midchord suction produced greater negative pressure-coefficient peaks at the leading edge of the model than were attained with the basic airfoil or the nose slot alone (reference 1). The change in chordwise loading produced by the midchord slot can be seen in these figures. The pressures at the trailing edge (fig. 6) recovered to greater than free-stream conditions, suggesting that no separation occurred even for an angle of attack of 21.1° ($c_l = 2.28$) near maximum lift. With the flap deflected 40° (fig. 7), the flow over the flap was separated throughout the angle-of-attack range.

Boundary-Layer Measurements

A typical set of boundary-layer-velocity profiles measured over the model with the flap undeflected is shown in figure 8. The conditions for these measurements were as near those corresponding to maximum lift as was practicable. Unsteadiness of flow rendered measurements at higher values of lift unsatisfactory. The chordwise variations of the derived boundary-layer parameters θ and H are shown in figure 9 for an angle of attack of approximately 12.7° for several slot configurations. The effect of increasing the angle of attack on these boundary-layer parameters for the model with both nose slot 2 and the midchord slot functioning is shown in figure 10.

The boundary-layer-velocity profiles shown in figure 8 show the stabilizing action of the midchord slot. The velocity close to the surface at the 49-percent-chord station, just ahead of the slot, was increased by the sink effect of the slot. Downstream of the slot the thickness of the boundary layer was greatly reduced. This same result is evident from the chordwise variations of the boundary-layer-momentum thickness θ and of the shape parameter H. Moreover, as would be expected, both the nose and the midchord suction slots reduced the values of both parameters below those for the basic wing. The effect of the midchord suction was more pronounced since the slot was located in a region where a relatively thick, well-developed, turbulent boundary layer existed.

Figure 10, which shows the effect of increasing the angle of attack, reveals that the value of the shape parameter at the trailing edge of the suction model near maximum lift was surprisingly low in comparison with the value 2.6, which has been shown to be indicative of turbulent separation. At a lift coefficient of 2.28 (the maximum lift coefficient, 2.39), the model was apparently in no imminent danger of stalling from separation of the turbulent boundary layer as is shown by the value of the shape parameter at the trailing edge (less than 1.6). This result leaves the cause of the stall uncertain. As mentioned previously, the flow over the model in the wind tunnel was irregular near the maximum lift, and undoubtedly was seriously affected by inflow from the tunnel-wall boundary layer which disrupted the two-dimensional nature of the flow.

For nose slot 1 (slot 15 of reference 1) with a flow coefficient of 0.0065, the addition of the midchord slot $(c_{q_B} = 0.0115)$ resulted in lift increments of approximately 0.30 and 0.20 with the flap undeflected and deflected 40°, respectively. These lift increases were accomplished without any apparent separation from either the leading or the trailing edge of the airfoil. It must be concluded, therefore, that for the investigation reported in reference 1, the stall of the airfoil with only the nose slot was due solely to turbulent separation from the trailing edge and not from the inability of the suction slot to maintain flow behind the leading edge.

Plenum-Chamber Pressures

An indication of the pressures against which the suction pumps must operate is given in figure 11. These data were obtained for the model with nose slot 2 from the average readings of static-pressure tubes in the plenum chambers. The pressures are expressed in the same manner as the pressure over the surface of the airfoil.

The smaller pressures in the nose-slot plenum chamber, as compared to those in the midchord-slot plenum chamber, were caused, primarily, by the low pressures in the vicinity of the leading edge against which the suction pump had to operate. A more efficient slot design would undoubtedly reduce the pressure ratio required to maintain suction through either of the slots. However, it is thought that any reduction in the required pressure ratio due to improved slot efficiency would be of secondary importance. The pressure field in which the slot is located will determine the basic pressure ratio.

It is interesting to note the suction power required by the nose and midchord slots. By the use of the following experimental values obtained at a Reynolds number of 4.1 million,

$$c_l = 2.8$$

$$c_{q_N} = 0.0065, \quad P = -24$$

$$c_{q_B} = 0.0115, \quad P = -1.6$$

and, with the assumption of ideal efficiency, a simple calculation of the suction power required for an airplane with a 10-foot-chord wing landing at 100 miles per hour gives

Nose slot, 10.7 horsepower per foot of span

Midchord slot, 1.3 horsepower per foot of span

Total, 12.0 horsepower per foot of span

Although the landing Reynolds number of the hypothetical airplane is considerably larger than 4.1 million and undoubtedly would affect the volume of the required suction flow, the example is presented to make the results directly comparable with the results of a similar calculation presented in reference 1.

CONCLUDING REMARKS

The combination of a nose and a midchord boundary-layer suction slot has been shown to be more effective in increasing the maximum lift of the NACA 63_1-012 airfoil section than a nose slot operating independently. For this investigation with the combined control, conducted at

Reynolds numbers of 5.8 and 4.1 million, the largest increments of the maximum section lift coefficients obtained were 1.01 with flap undeflected and 0.84 with the flap deflected 40°. These values are larger by 0.39 and 0.30, respectively, than those obtained with the nose slot alone. Greater volume flows through the slots than those which were attainable with the experimental apparatus appear to offer still greater effectiveness.

Because of the greater values of lift attained by the model with combined suction, it is clear that the nose slot of the model without a midchord slot was capable of preventing leading-edge separation for conditions of pressure minimum and pressure gradient more severe than those encountered in the investigation of the model without a midchord slot. The cause of the stall with combined leading-edge and midchord suction was uncertain. Because the boundary-layer measurements over the model midspan gave no indication of any pending flow separation, it is thought that the maximum lift of the model in the wind tunnel was limited by a breakdown of two-dimensional flow due to tunnel-wall boundary-layer bleeding into the boundary layer of the model.

Ames Aeronautical Laboratory,
National Advisory Committee for Aeronautics,
Moffett Field, Calif., November 17, 1949.

REFERENCES

1. McCullough, George B., and Gault, Donald E.: An Experimental Investigation of an NACA 63_1-012 Airfoil Section with Leading-Edge Suction Slots. NACA TN 1683, 1948.

2. Allen, H. Julian, and Vincenti, Walter G.: Wall Interference in a Two-Dimensional-Flow Wind Tunnel with Consideration of the Effect of Compressibility. NACA Rep. 782, 1944.

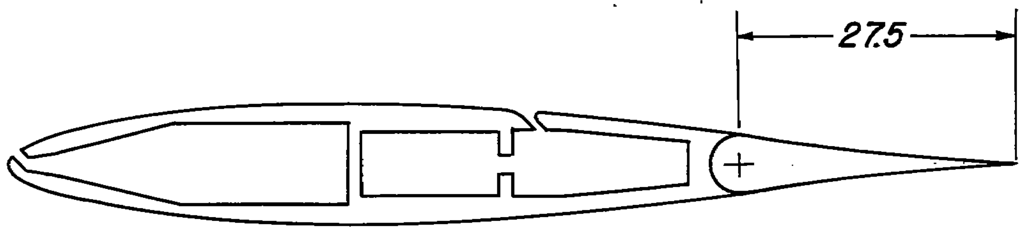

Typical section

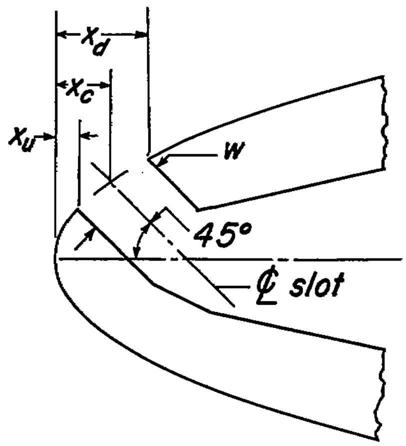

Slot	x_u	x_c	x_d	w
1	0.377	0.667	1.000	0.800
2	.377	.900	1.533	1.400

Note: All dimensions are in percent of wing chord

Nose slot

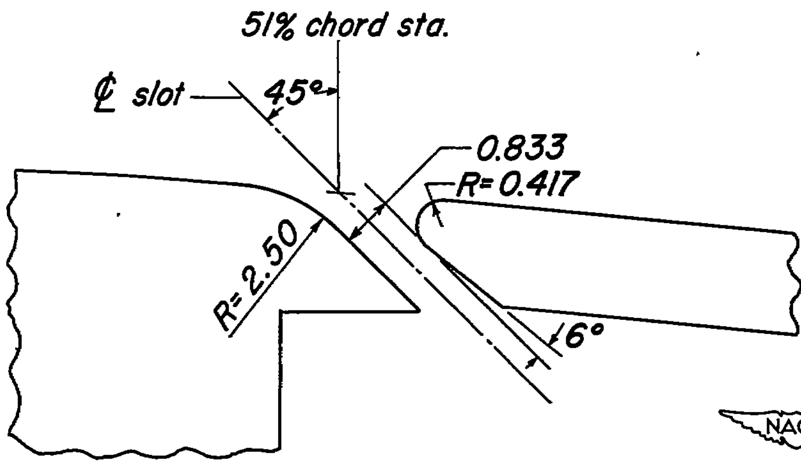

Midchord slot

Figure 1.- Geometry of the model and the slots.

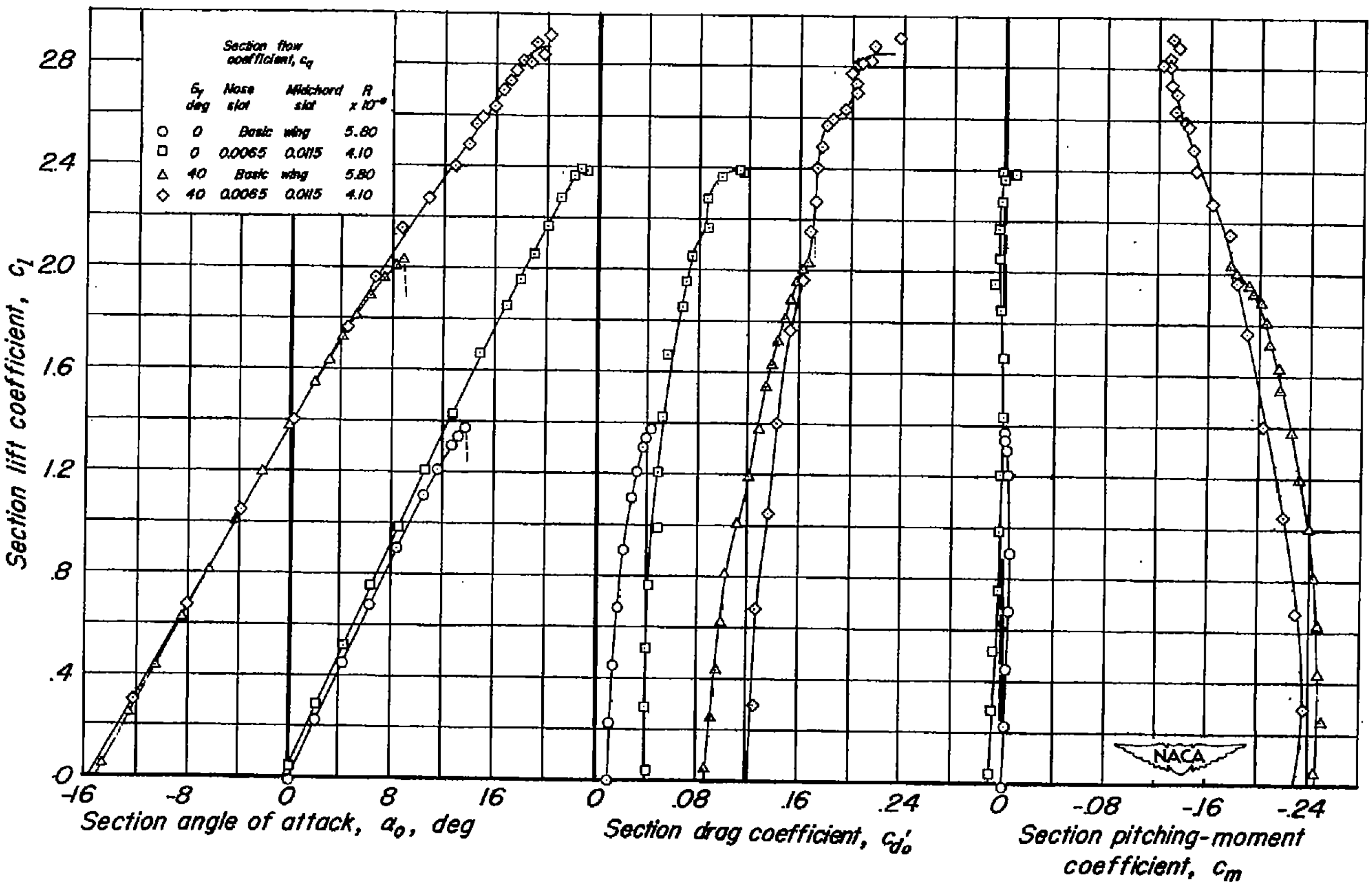

Figure 2.—Typical lift, drag, and pitching-moment characteristics from balance-system measurements of the model with slot 2 and midchord slot.

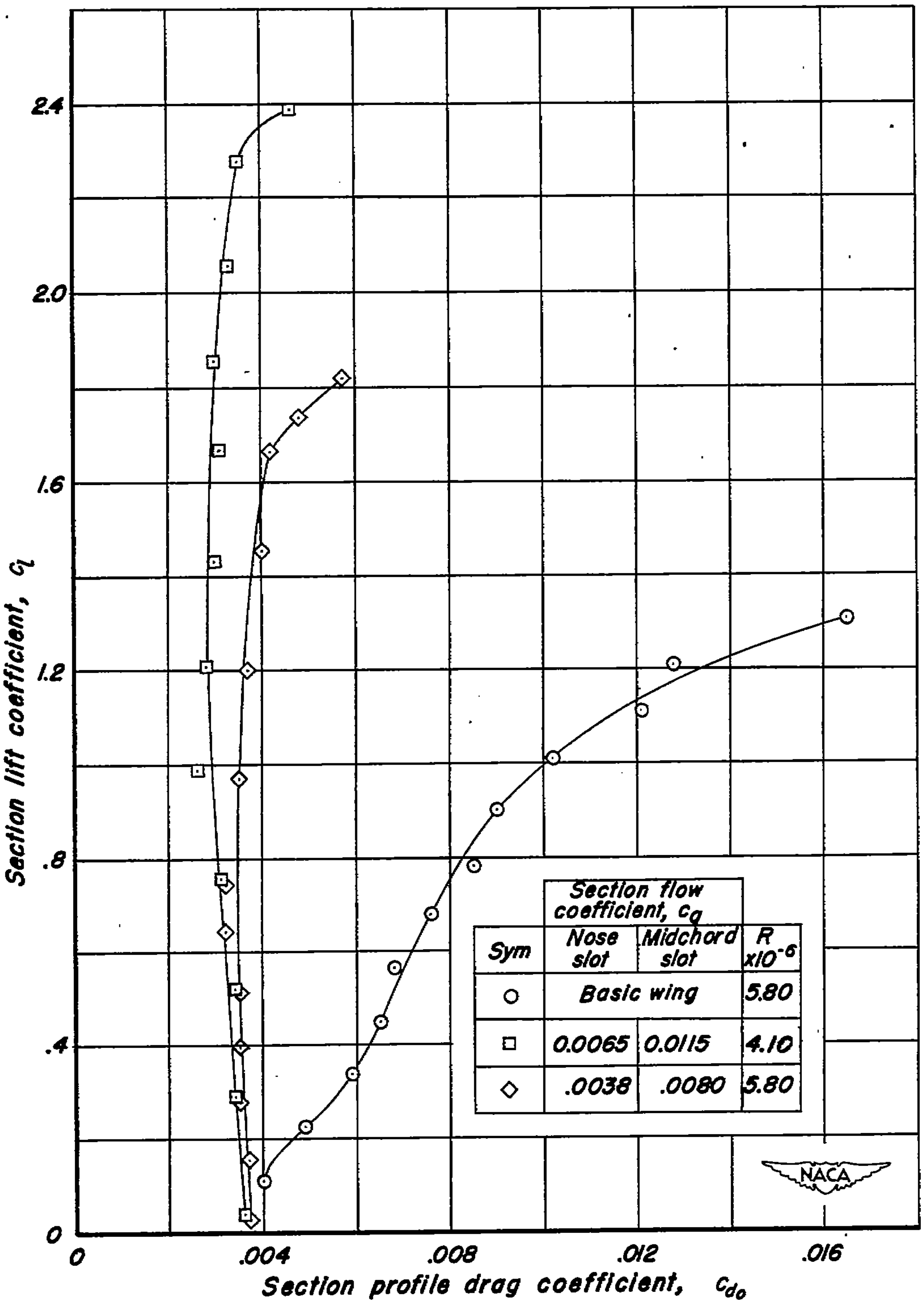

Figure 3.-Variation with lift coefficient of profile drag coefficient determined from wake surveys for the model with slot 2 and midchord slot.

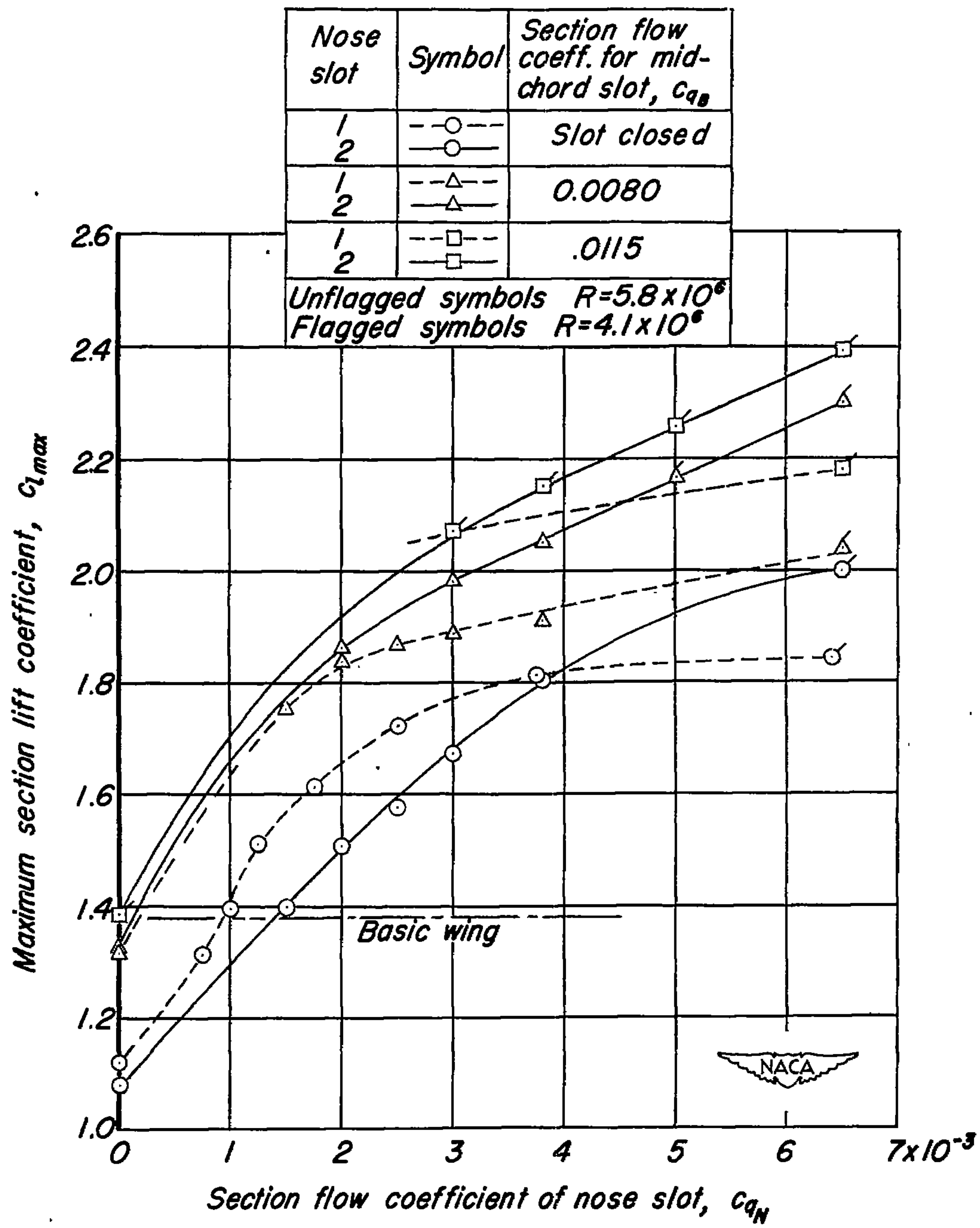

Figure 4.-Variation of maximum lift coefficient with flow coefficient for the model with flap undeflected.

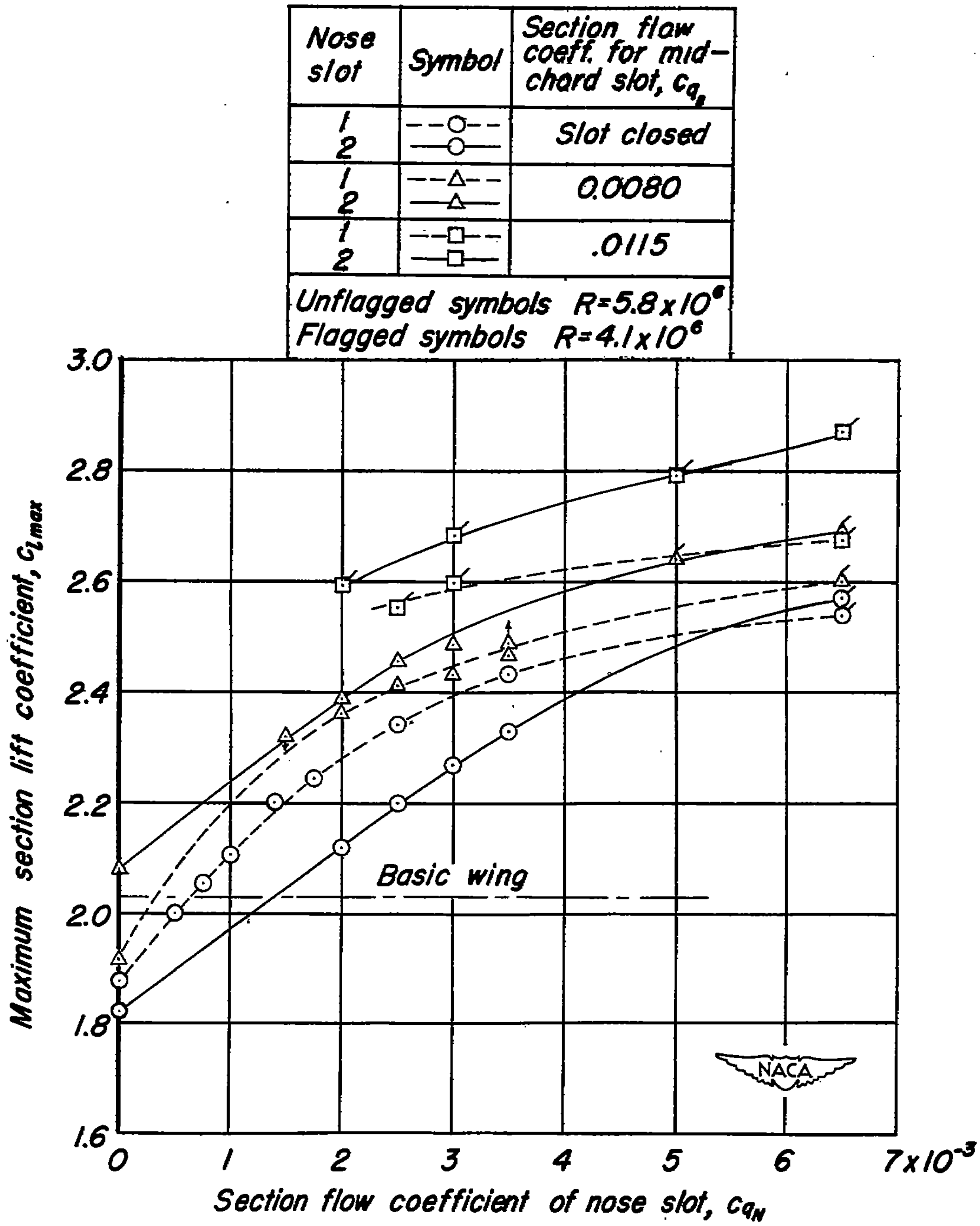

Figure 5.–Variation of maximum lift coefficient with flow coefficient for the model with flap deflected 40°.

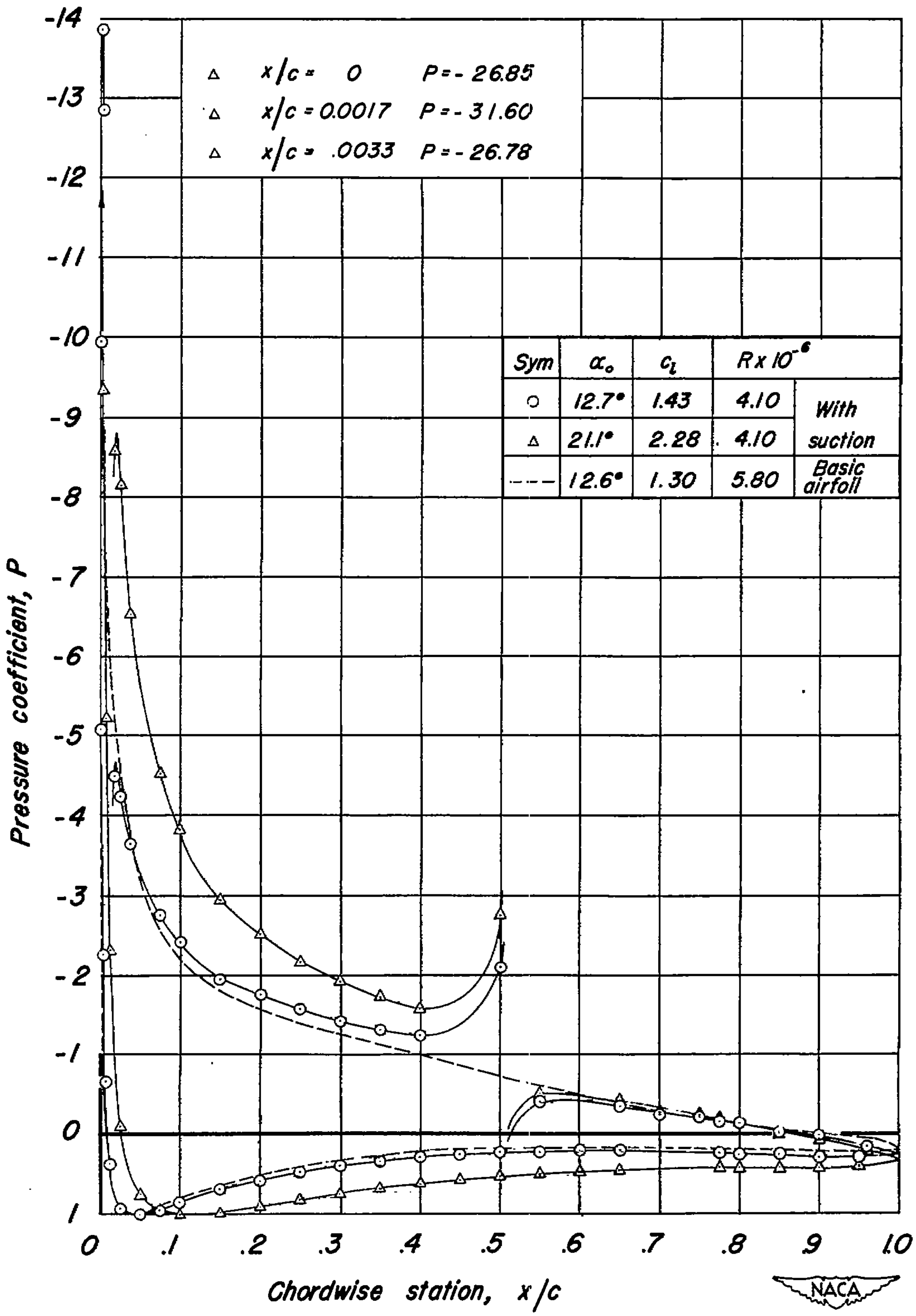

Figure 6.- Pressure distributions for the model with flap undeflected. Slot 2; c_{q_N} = 0.0065; c_{q_B} = 0.0115.

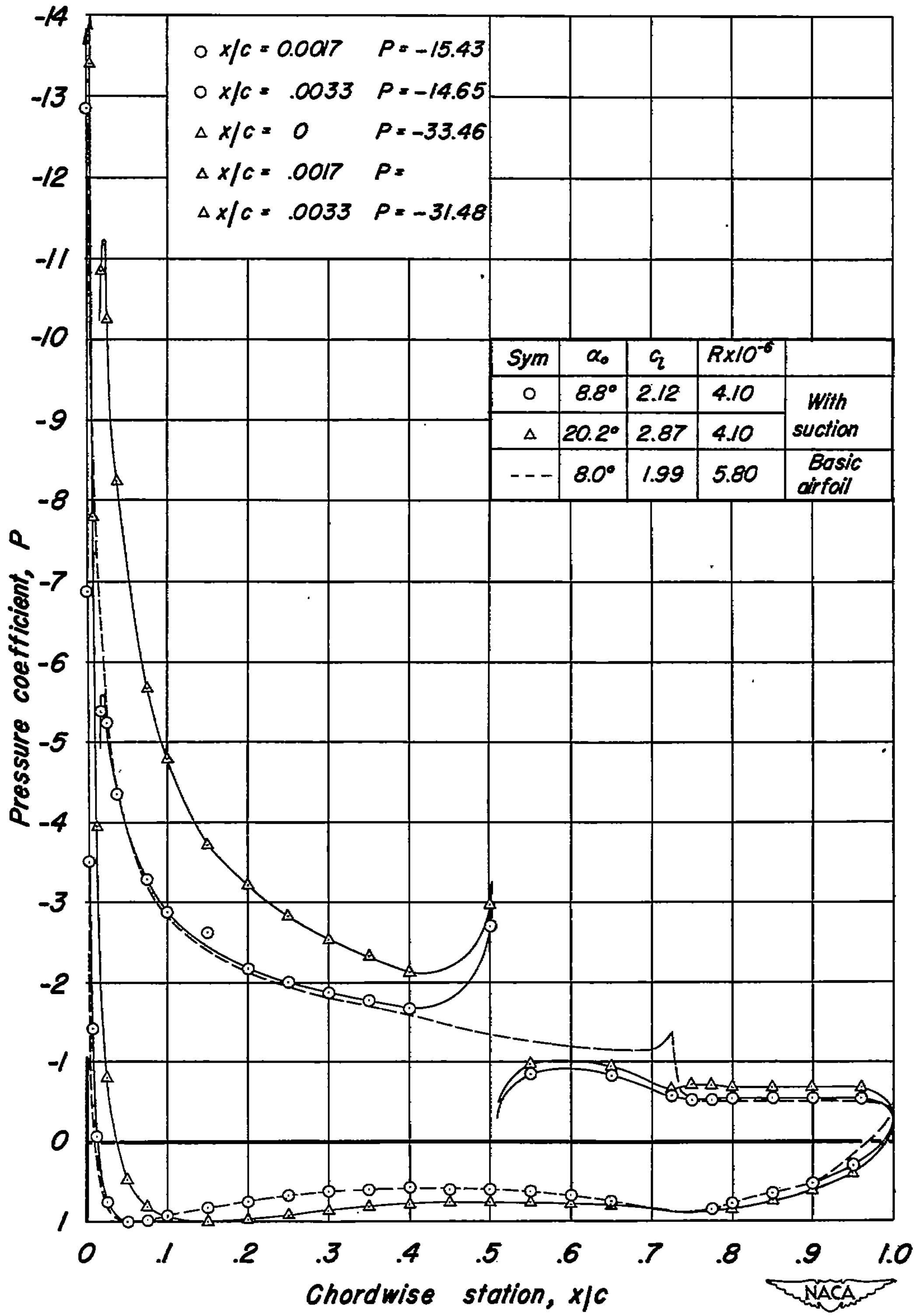

Figure 7.–Pressure distributions for the model with flap deflected 40°. Slot 2; $c_{q_N} = 0.0065$; $c_{q_B} = 0.0115$.

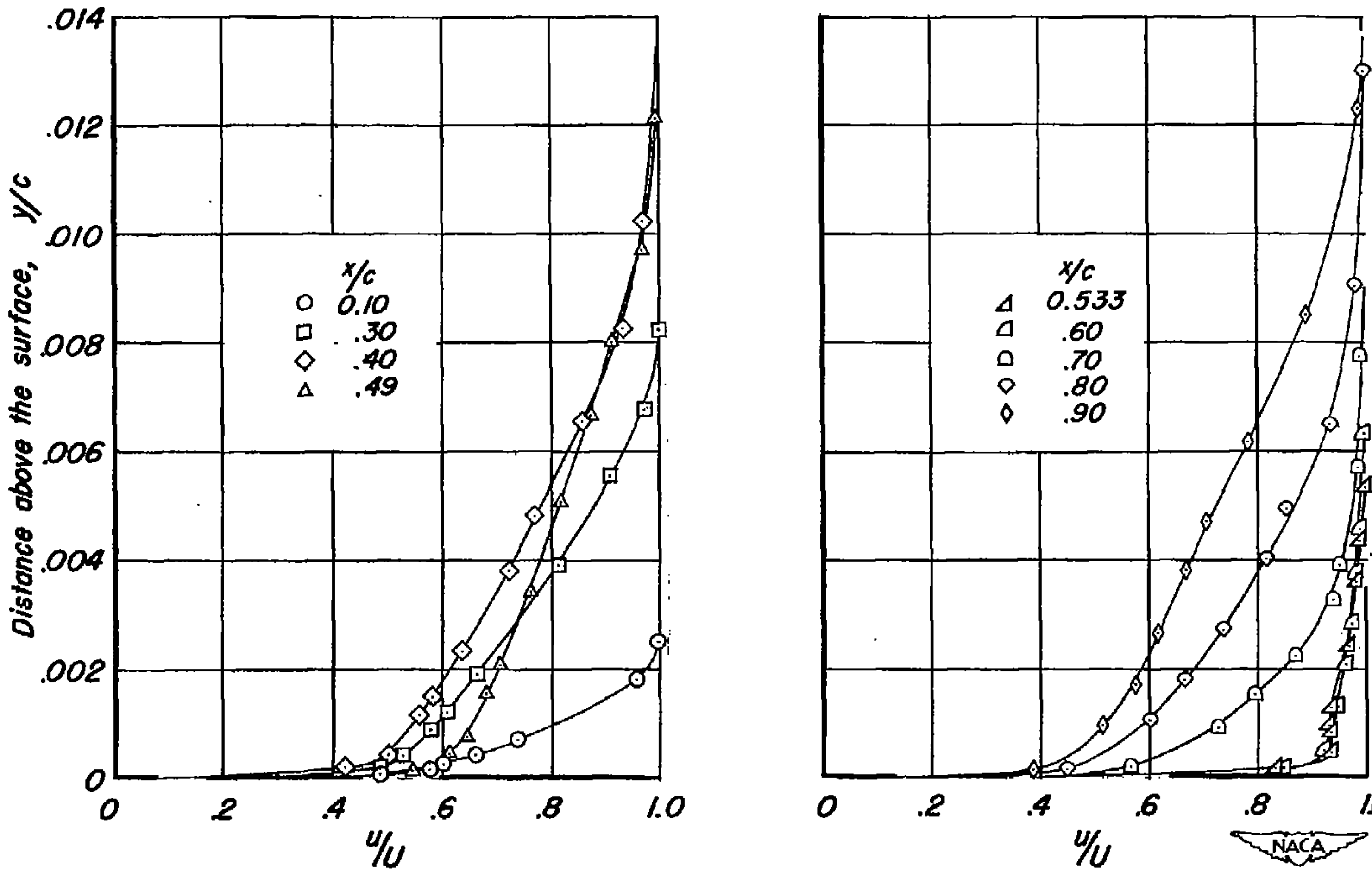

Figure 8.–Typical boundary-layer-velocity profiles. Slot 2; $c_{q_N} = 0.0065$; $c_{q_B} = 0.0115$; $\alpha_o = 21.1°$; $c_L = 2.28$, $R = 4.1 \times 10^6$.

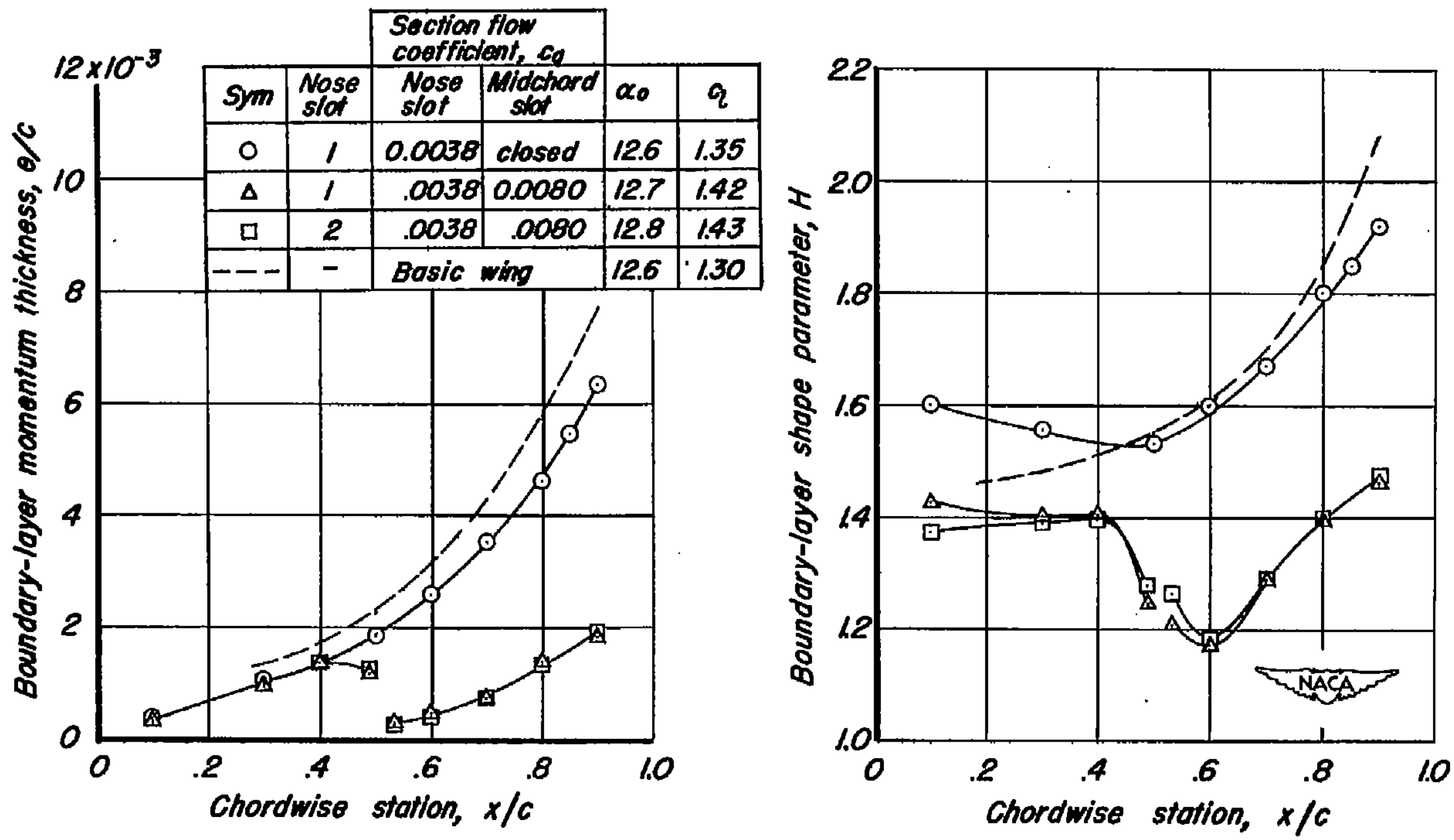

Figure 9.–The effect of slot configuration on the chordwise variation of the boundary-layer momentum thickness and shape parameter. $R = 5.8 \times 10^6$.

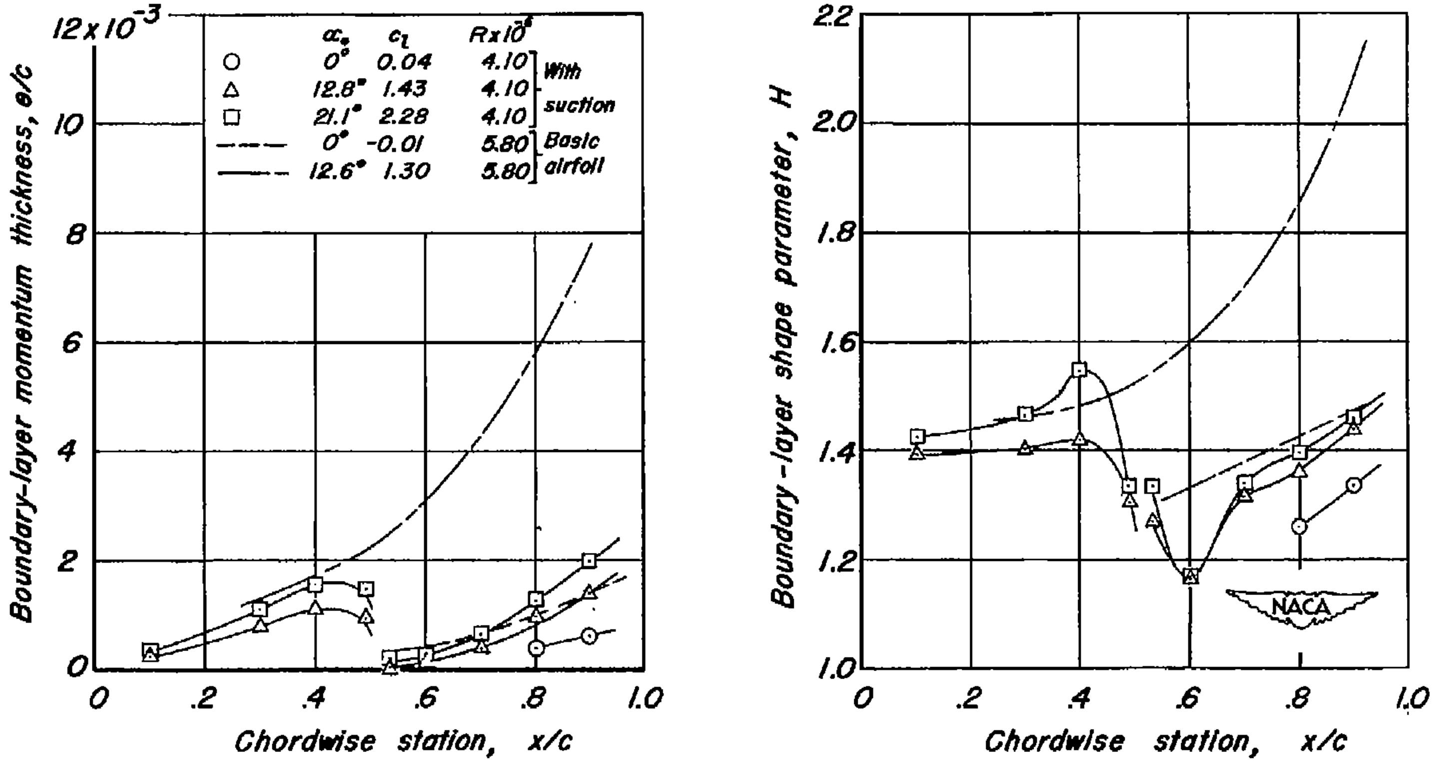

Figure 10.–The effect of angle of attack on the boundary-layer momentum thickness and shape parameter for the model with slot 2 and midchord slot. $c_{q_N} = 0.0065$; $c_{q_B} = 0.0115$.

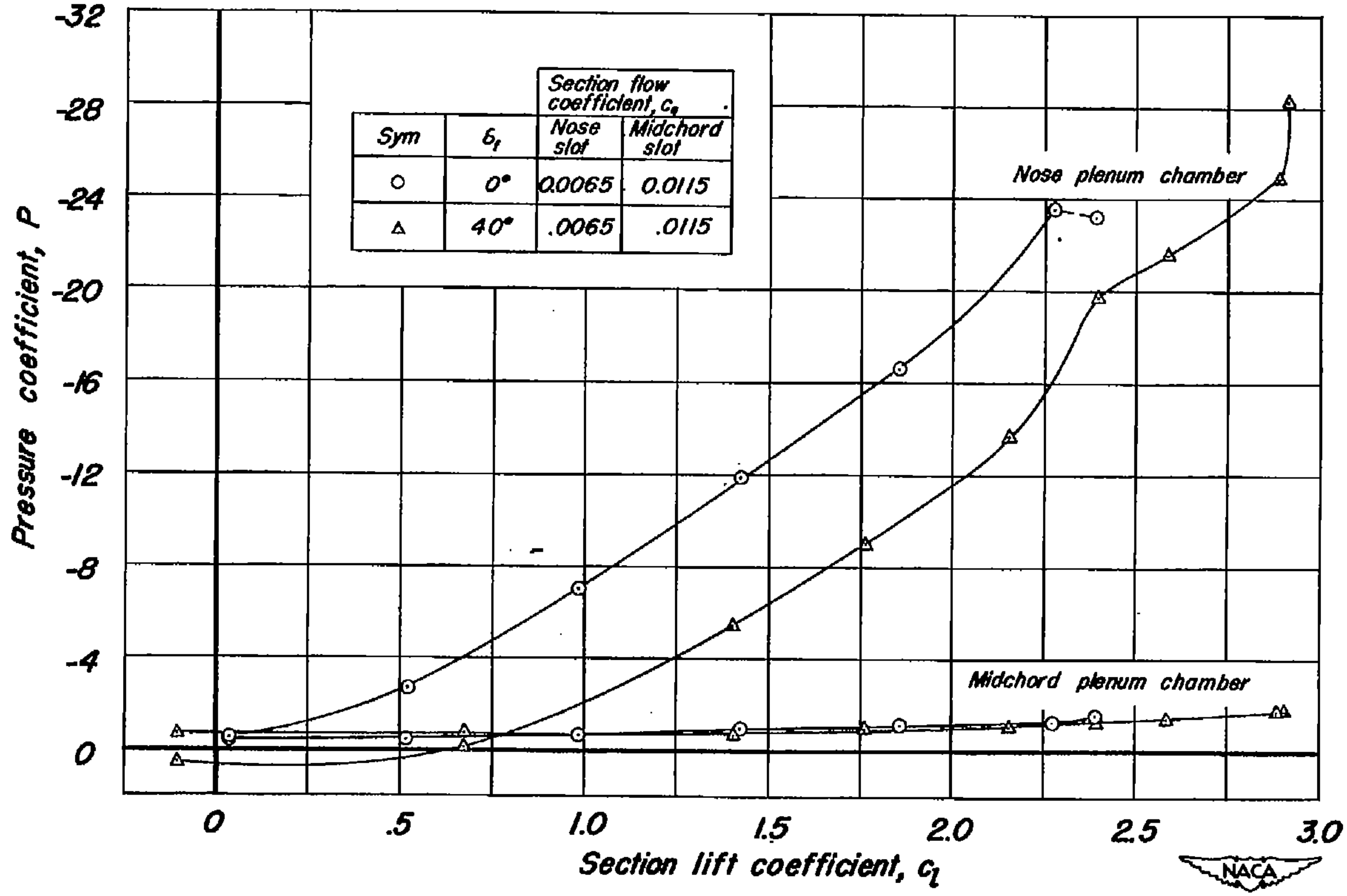

Figure 11.—Plenum-chamber pressures for the model with slot 2 and midchord slot. $R = 4.1 \times 10^6$.

NACA-Langley - 3-2-50 - 200